RF DESIGN OF THE 1 kHz PHOTOINJECTOR FOR THE RUEDI ELECTRON DIFFRACTION FACILITY

L. S. Cowie*, A. J. Gilfellon, B. R. Hounsell, B. L. Militsyn, J. W. McKenzie,
T.C.Q. Noakes, S. S. Percival, UKRI STFC Daresbury Laboratory, Warrington, UK
G. Burt, Lancaster University, Lancaster UK

Abstract

The RUEDI RF photoinjector will have a 2.45 cell S-band gun producing electrons at 4 MeV. The gun is designed to operate at 1 kHz repetition rate. This will be achieved by a combination of RF over-coupling to reduce the RF pulse length, and an advanced water cooling system based on that of the CLARA 400 Hz photoinjector. The shorter pulse length is also intended to limit the dark current, along with operation at 70 MV/m, and the use of a flat back plate cathode. The cell lengths are optimised to improve jitter cancellation performance, as well as to limit surface electric fields on the irises. The cavity is dual side-coupled into the middle cell with a racetrack coupling cell to reduce the quadrupole component of the RF field, and has an RF probe on the final cell.

INTRODUCTION

RUEDI (Relativistic Ultrafast Electron Diffraction & Imaging) is a proposed user facility to be based at Daresbury Laboratory [1, 2], with a diffraction line that will deliver ultrafast electron diffraction down to 10 fs timescales and an imaging line for single-shot, time-resolved imaging with MeV electrons. The diffraction line will consist of a 2.45 cell S-band RF photoinjector with a magnetic compression arc and variable diffraction optics [3]. The interaction region will have a large variety of pumps and sample environments and electron bunch diagnostics. The RF design of the RUEDI photoinjector for the diffraction line is presented here.

CAVITY GEOMETRY DESIGN

The photoinjector is a 2.45 cell S-band (2998.5 MHz RF gun, with a Ti:sapphire laser producing UV pulses at the third-harmonic wavelength 266 nm. It will have a focusing solenoid after the cavity, 0.22 m from the cathode. S-band was chosen due to it being a well-developed technology with easily available power sources and transport. It also allows high enough RF fields to operate in the beam-blowout regime [4]. The bunches will be long (188 fs RMS) at the exit of the gun but will be compressed to under 10 fs at the sample in a magnetic compression stage. The magnetic compressor will also suppress the time of flight jitter to the sample to below 10 fs [5]. The fields, however, will be low enough to minimise dark current whilst still reaching the full RUEDI kinetic energy of 4 MeV in a single RF cavity. Operation at 70 MV/m reduces the theoretical dark current by 92% compared to 100 MV/m [6]. In the 2.45 cell CLARA photoinjector, which operates at a similar cathode field, it was found that the most problematic dark current was mostly from the edge of the vacuum-interchangeable cathode plug, and from the rim around the plug opening [7]. For this reason for RUEDI the copper back plate will serve as the cathode; it will be exchangeable, but not under vacuum.

The gun design, including a racetrack coupling cell, is shown in Fig. 1. Side power coupling was chosen to allow both a large aperture for the photoinjector laser transport at near-normal incidence and optimal solenoid placement. Z-coupling with rounded slots will reduce the fields on the coupler opening. Elliptical irises between the cells minimise the surface fields. The shortest major radius (iris thickness) that would allow the same cooling design as the CLARA 400 Hz photoinjector is 8 mm [8], and was chosen to maximise shunt impedance. The iris radius (from the beam axis) is 14.5 mm to give a mode separation of greater than 15 MHz, with the final iris radius 15 mm to allow photoinjector laser transport.

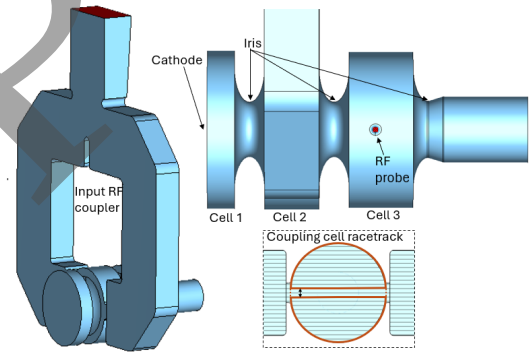

Figure 1: Final RF design geometry.

A racetrack shaped coupling cell minimises the quadrupole component from the dual waveguide coupler. This can be seen in Fig. 2, which shows the electric field E_z in the z direction around a 3 mm radius circle around the z axis in the coupling cell for three racetrack lengths. A 4 mm straight on the cell equator reduces the quadrupole component to below the simulation noise level. GPT [9] simulations show that a 4 mm racetrack decreases the difference in vertical and horizontal normalised RMS emittance (transverse emittance asymmetry) from 13.7 to 1.7 nm · rad compared to a round cell for a bunch with approximate total transverse emittance 40 nm · rad. The gun design also includes a probe on the third cell; it has −67.2 dB coupling and is symmetrised by using a dummy probe port opposite.

* louise.cowie@stfc.ac.uk

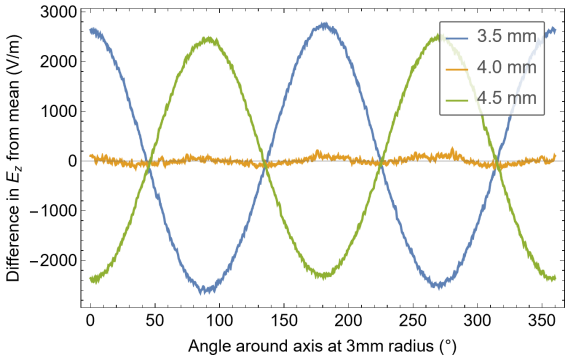

Figure 2: The quadrupole component is minimised with a 4 mm straight on the racetrack cell.

Initial optimisation of the half cell showed that a cell length ratio of 0.4:1:1 achieved a lower RMS longitudinal emittance and bunch length, along with better jitter suppression characteristics. Subsequent optimisation included varying the second cell length, as the beam is not fully relativistic in this cell. The final cell length ratio is 0.45:0.9:1; this has the effect of reducing the peak electric field on the first iris to below the cathode field. This cell length ratio also shows better correlation between the phase and amplitude energy-time jitters across the whole range of operational phases. This means that the R56 required to suppress the time of flight jitter using the magnetic compression stage is similar for phase and amplitude, leading to smaller overall timing jitter at the interaction point over a wide range of operational phases. The required R56 for suppression of time of flight jitter due to amplitude jitter and phase jitter against gun operating phase for the initial and final designs can be seen in Fig. 3.

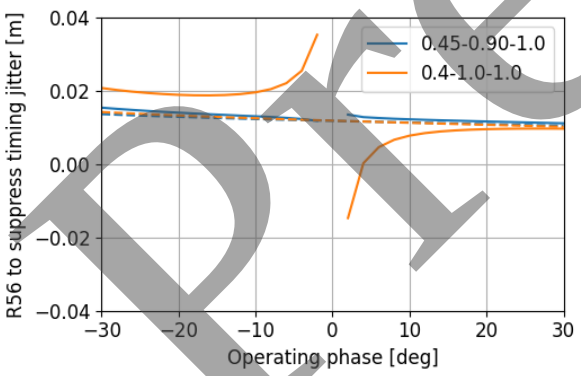

Figure 3: Required R56 for suppression of time of flight jitter due to amplitude jitter (dashed) and phase jitter (solid) against gun operating phase for two cell length ratio designs.

PULSE LENGTH AND SHAPE

A short RF pulse length, along with the lower cathode field, keeps the average power dissipation low to allow a high repetition rate of 1 kHz; the short pulse length will also minimise dark current. The RF coupling factor (β) was optimised to minimise the time to reach an effective voltage of 4 MV with 7 MW input power (using a 10 MW klystron). The coupling factor is 2 and the pulse length is 1.05 µs.

The pulse shape was studied. A stepped input RF pulse shape can be used to achieve a voltage flat top. For the planned single bunch operation there is a choice, which will be made experimentally: a square pulse would allow the whole pulse to be amplified by the klystron in saturation, which can reduce any jitter caused by LLRF timing combined with modulator voltage intra-pulse fluctuation. However, a stepped pulse gives a flat top in gun voltage, which would reduce the effect of any laser-RF timing jitter. It should be noted that the main source of jitter is expected to be the modulator voltage stability and this is unaffected by pulse shape, but a potential future upgrade to analogue intra-pulse feedback is being considered [10].

Pulse shape optimisation was simulated with an equivalent circuit model and Fourier methods to find the reflected power and effective voltage pulse shapes for an arbitrary input pulse. The single-cell RLC circuit model was used to find an equation for reflectance Γ as a function of frequency ω:

$$\Gamma(\omega) = \sqrt{\frac{P_r}{P_f}}\frac{\beta - 1 - i\gamma(\omega)}{\beta + 1 + i\gamma(\omega)}e^{i\phi} \tag{1}$$

where $\gamma = Q_0(\frac{\omega_0}{\omega} - \frac{\omega}{\omega_0})$, ω_0 is the resonant frequency, Q_0 is the unloaded quality factor, P_r and P_f are the reflected and forward powers, β is the coupling factor, and ϕ is the phase. Equivalent circuit modelling was also used to find the effective voltage V_{eff} as a function of frequency:

$$V_{eff}(\omega) = \sqrt{P_f R_{eff}}\frac{2\beta^{1/2}}{1+\beta}\frac{e^{i\phi}}{1+\gamma_L(\omega)} \tag{2}$$

where $\gamma_L = iQ_L(\frac{\omega_0}{\omega} - \frac{\omega}{\omega_0})$ Q_L is the loaded quality factor and R_{eff} is the effective shunt impedance.

The Fourier transform of an arbitrary pulse shape can then be multiplied by the frequency-dependent reflectance in the frequency domain; an inverse Fourier transform gives the reflected power as a function of time. The same can be done with the frequency-dependent effective voltage to give the time-dependent voltage. The two options for pulse shaping are shown in Fig. 4.

SURFACE MAGNETIC FIELDS AND HEATING

The pulsed heating temperature rise for each magnetic field hot-spot was estimated using

$$\Delta T = \frac{R_s H^2 \sqrt{\tau}}{\sqrt{\pi \rho\, k c_e}}, \tag{3}$$

where R_s is the surface resistance, ρ is the density, k is the thermal conductivity, c_e is the specific heat of the material, and τ is the pulse length [11]. This calculation gives modest temperature rises, well under the 40 K damage limit as shown in Table 1. The mechanical design will include further analysis of stress and deformation.

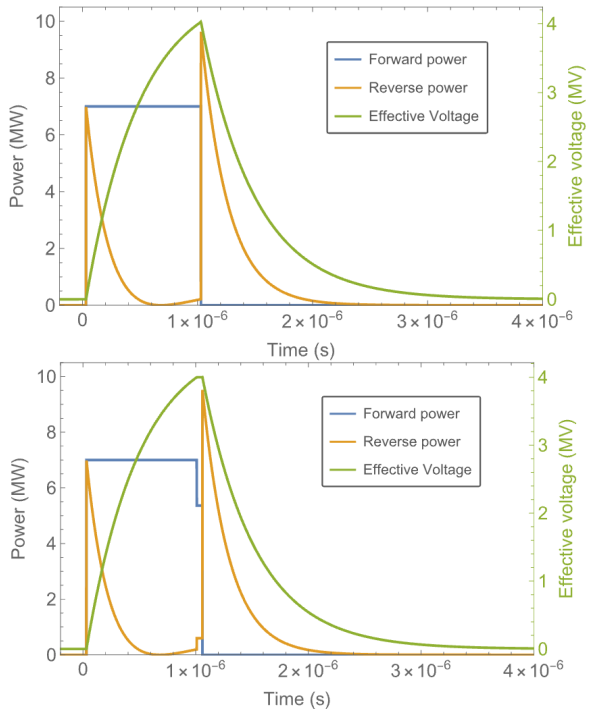

Figure 4: Pulse shaping for β=2 cavity with square (top) or stepped input pulse (bottom).

Table 1: Calculated Pulsed Heating Temperature Rises

Location	Field (kA/m)	Temp. rise (K)
Coupling slot	251	14.5
Probe tip	75	1.3
Probe edge	98	2.2

From simulation the average power dissipation was calculated for each possible operational repetition rate; these are 408 W for 100 Hz, 816 W for 200 Hz, and 4077 W for 1 kHz. The cooling system for the CLARA 400 Hz photoinjector has 6.8 kW power dissipation [8] so a similar cooling system is planned for RUEDI. The probe in the third cell will be used for pulse-to-pulse temperature feedback.

MULTIPACTOR SIMULATION

Simulations in SPARK3D [12] show a risk of multipactor at cathode fields between 10 MV/m and 60 MV/m. Comparison with the theoretical estimation of multipactor at the equator agrees with the SPARK3D simulations well. The approximate strength of the local magnetic field B_0 with multipactor order n is given by

$$B_0 = \frac{2\pi\nu m_0}{e}\frac{1}{n}, \tag{4}$$

where ν is the RF frequency, e the electron charge and m_0 the electron rest mass [13]. The comparison between SPARK3D and the estimated equatorial multipactor order can be seen in Fig. 5. There is no multipactor seen in simulation at the planned operating cathode field of 70 MV/m; however the multipactor at 60 MV/m may be of concern if the field is reduced for lower beam energy experimentation. Operation at this field is not foreseen at this time, and the multipactor may process away to potentially allow operation in this region, as has been the experience on CLARA.

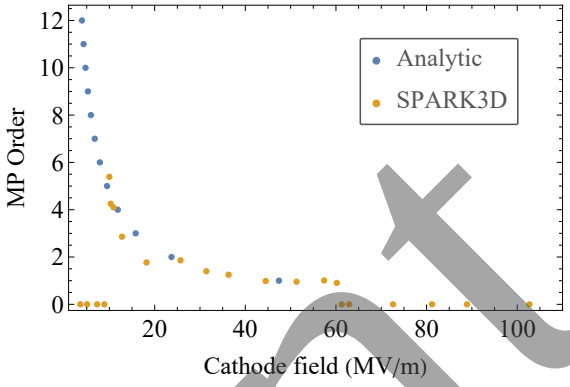

Figure 5: Comparison of SPARK3D simulation and theoretical estimate for equatorial multipactor.

FIELD FLATNESS TUNING

The gun is designed to have the same peak field in each cell, but manufacturing tolerances in the radii or irises of the first half-cell and the final cell can affect this field flatness. The cavity cells will be manufactured with extra length on these two cells, which can then be trimmed to the length that will correct the field flatness. This will be done based on clamped low power RF bead-pull measurements, as was done for the CLARA 400 Hz photoinjector [14]. An algorithm has been written in Python to predict the cell lengths required, given the measured field flatness, and tested with randomised simulated radial errors. These radial errors of up to ± 20 µm cause field flatness variations up to 22%. Adjusting the cell lengths in the simulation to compensate for the randomised errors show that the field flatness variations are reduced to within 3%.

CONCLUSION AND FURTHER WORK

The RF design for the RUEDI photoinjector is presented. It has several novel features that make it highly specialised for electron diffraction experiments, when combined with a magnetic compression arc:

- Jitter suppression to sub-10 fs level enabled by optimised first half-cell and second cell lengths, allowing jitter compensation for phase and amplitude in the arc;
- 1 kHz operation enabled by over-coupling, 70 MV/m cathode field and advanced water cooling scheme;
- Reduced risk of high dark current due to 70 MV/m cathode field and flat copper cathode.

Further work will focus on the mechanical design. This will include manufacturing drawings, cooling system design based on CLARA gun-400 and able to manage heat loads of 5 kW, and finite-element simulations of temperature, stress and deformation.

REFERENCES

[1] J. McKenzie *et al.*, "Establishing a relativistic ultrafast electron diffraction and imaging (RUEDI) UK national facility", in *Proc. IPAC'23*, Venice, Italy, May 2023, pp. 2075–2078. doi:10.18429/JACoW-IPAC2023-TUPL144

[2] J. McKenzie *et al.*, "Status of the RUEDI UK national facility design", in *Proc. IPAC'24*, Nashville, TN, USA, May 2024, pp. 1979–1982. doi:10.18429/JACoW-IPAC2024-WEPC13

[3] S.Percival *et al.*, "Variable sample illumination and angular magnification for the RUEDI ultrafast electron diffraction beamline", presented at IPAC'26, Deauville, France, May 2026, paper THP2128, this conference.

[4] O. J. Luiten *et al.*, "How to realize uniform three-dimensional ellipsoidal electron bunches", *Phys. Rev. Lett.*, vol. 93, no. 9, p. 094802, Aug. 2004. doi:10.1103/PhysRevLett.93.094802

[5] B. Hounsell *et al.*, "An update of progress on the design of the diffraction line for the relativistic ultrafast electron diffraction and imaging facility at Daresbury Laboratory", in *Proc. IPAC'25*, Taipei, Taiwan, Jun. 2025, pp. 1208–1211. doi:10.18429/JACoW-IPAC2025-TUPM021

[6] R. H. Fowler and L. Nordheim, "Electron emission in intense electric fields", *Proc. R. Soc. Lond. A*, vol. 119, no. 781, pp. 173–181, May 1928. doi:10.1098/rspa.1928.0091

[7] F. Jackson *et al.*, "Characteristics of dark current from an S-band rf gun with exchangeable photocathode system", *arXiv*, 2025. doi:10.48550/arXiv.2403.00700

[8] J. W. McKenzie *et al.*, "High Repetition Rate S-band Photoinjector Design for the CLARA FEL", in *Proc. FEL'14*, Basel, Switzerland, Aug. 2014, Aug. 2014, paper THP064, pp. 889–892.

[9] M. J. de Loos and S. B. van der Geer, "General Particle Tracer: A New 3D Code for Accelerator and Beamline Design", in *Proc. EPAC'96*, Sitges, Spain, Jun. 1996, Jun. 1996, paper THP001G, pp. 1241–1243.

[10] L. Piersanti *et al.*, "Design and test of a klystron intra-pulse phase feedback system for electron linear accelerators", *Photonics*, vol. 11, no. 5, p. 413, 2024. doi:10.3390/photonics11050413

[11] D. P. Pritzkau, "RF pulsed heating", Ph.D. thesis, Stanford University, California, Jan. 2001.

[12] Dassault Systemes, SPARK3D, 2025. https://www.3ds.com/products/simulia/spark3d

[13] R. F. Parodi, "Multipacting", *arXiv*, 2011. doi:10.5170/CERN-2011-007.447

[14] L. S. Cowie, "Normal conducting RF structure development for CLARA", Ph.D. thesis, Lancaster University, UK, 2022.